Magnetic Hardening of $Sm_2Fe_{17}N_3$ by Radiation Damage

N. M. Dempsey,[1] M. Ghidini,[2] J. P. Nozières,[3] P. A. I. Smith,[1] B. Gervais,[4] and J. M. D. Coey[1]
[1]*Department of Physics, Trinity College, Dublin 2, Ireland*
[2]*Dipartimento di Fisica dell'Universit di Parma e INFM, Parma, Italy*
[3]*Laboratoire Louis Néel, CNRS, Grenoble, France*
[4]*CIRIL, Caen Cedex, France*
(Received 6 July 1998)

Pinning type coercivity has been induced in large ($\approx$50 μm) particles of $Sm_2Fe_{17}N_3$ by irradiation with 5 GeV Pb^{56+} ions. Mössbauer spectroscopy is used to analyze the structure of the defects and estimate their volume. Magnetization measurements indicate that the induced defects are anisotropic in shape. A model of strong pinning by cylindrical defects is employed to deduce a defect radius of order 2 nm from the measured fluence dependence of the coercivity. [S0031-9007(98)07898-3]

PACS numbers: 75.50.Ww, 61.80.Jh, 75.50.Vv

The fully magnetized state of a ferromagnet is usually metastable. For particles larger than a certain critical size d_c, which is of order 1 μm, the zero field equilibrium state is a multidomain configuration with no net magnetization. In order to make a permanent magnet from powder with a particle size larger than d_c, both strong uniaxial anisotropy and a specific microstructure are required to obtain energy barriers to magnetization reversal [1]. Two strategies are available to produce the energy barriers: One is to impede nucleation of reverse domains and the other is to prevent the propagation of reverse domains by pinning the domain walls at defects in the hard phase. These defects should be extended as the pinning force is proportional to the area of wall passing through the defects, and they should have a thickness comparable to the domain wall width δ_w, which is typically a few nanometers [2]. Most modern magnets are of the nucleation type; only in Sm-Co-Fe-Cu-Zr "2:17"-type alloys has it proved possible to achieve pinning in a microstructure consisting of a network of rhombohedral cells separated by thin Cu-rich layers of the required width [3].

Swift heavy ions have a penetration depth in metals of order 10–100 μm, where they leave a trail of radiation damage. One area where they have been used to great effect is the pinning of vortices in type-II superconductors [4]. Another is in garnet films, where coercivity has been induced by etching the latent tracks to create cylindrical voids [5]. Amorphous ferromagnetic nanodomains with perpendicular anisotropy have been written in nonmagnetic crystalline films [6].

Here we present the first account of magnetic hardening in a permanent magnet material by radiation damage. The material chosen is $Sm_2Fe_{17}N_3$, which has good intrinsic magnetic properties, including easy c-axis anisotropy with an anisotropy field of 14 T at room temperature; d_c is 0.4 μm and δ_w is 3.6 nm [7]. However, coarse-grained powder (grain size $>$10 μm) shows very little coercivity. This is probably due to inclusions of α-Fe which precipitate from the metastable nitride during the nitrogenation process and act as nucleation centers for magnetization reversal.

Sm_2Fe_{17} powders were obtained by pulverizing induction melted ingots in a ball mill. Scanning electron microscopy investigations revealed that the starting ingots had grain sizes of 50–200 μm and traces of a Sm-rich impurity phase. The powder was nitrided in a flowing mixed gas NH_3/H_2 atmosphere [8,9]. To prepare samples for ion irradiation, 20 or 50 μm powder was mixed with epoxy resin (2:1 by weight) and sandwiched between two 15 μm sheets of Al foil. The thickness of the powder and epoxy mixture was then reduced to 50 μm by lamination in a roller mill. Aligned samples were prepared with the finer powder by curing the epoxy sandwich in a magnetic field of 0.6 T.

Square sandwiches (16 mm^2) were irradiated with a 5 GeV Pb^{56+} ion beam at the GANIL accelerator in Caen, France. The total fluence ranged from 10^{11} to 2×10^{13} ions/cm^2. The penetration depth of the ions in the magnetic material was estimated from calculations using TRIM (transport of ions in matter) code [10] to be approximately 100 μm.

Room temperature ^{57}Fe Mössbauer spectra of a reference $Sm_2Fe_{17}N_3$ powder, and samples irradiated at high fluences are shown in Fig. 1(a). In the reference, about 3% of a paramagnetic phase was detected in addition to the four subspectra of $Sm_2Fe_{17}N_3$ [11]. The spectra of the irradiated samples have a greater paramagnetic contribution and a broad ferromagnetic contribution characteristic of an amorphous or strongly disordered phase. The spectra of the irradiated samples were fitted with an additional paramagnetic doublet and a distribution of ferromagnetic subspectra, from which the percentage of Fe atoms in the damaged regions were determined. For the maximum fluence of 2×10^{13} ions/cm^2 this fraction was 51%. In the samples irradiated with fluences of 5×10^{12} and 1×10^{13} ions/cm^2, it was estimated that 23% and 28%, respectively, of all Fe atoms were in the damaged regions.

 0031-9007/98/81(25)/5652(4)$15.00

The absorption due to the radiation-damaged region, shown in Fig. 1(b), was obtained by stripping the normal $Sm_2Fe_{17}N_3$ spectrum. The shape of the resultant spectrum could be accounted for by a broad distribution of hyperfine fields, or by magnetic relaxation with a relaxation time of approximately 10^{-9} s. At low temperatures (26 K), the magnetically split absorption increases relative to the broad doublet, which could reflect an increased relaxation time, or the existence of a broad distribution of Curie temperatures (consistent with a broad distribution of hyperfine fields). The absorption due to the damaged regions, however, remains practically unchanged at 48% of the total for $\phi = 2 \times 10^{13}$ ions/cm^2.

If each ion creates a continuous cylindrical defect, the fraction P of the target damaged by irradiation, allowing for track overlap, is

$$P = 1 - \exp(-\pi r^2 \phi), \tag{1}$$

where r is the radius of the cylindrical defect and ϕ is the total ion fluence. The value of P for a fluence of 2×10^{13} ions/cm^2 is estimated from the Mössbauer spectra to be 51%. It follows from (1) that $r = 1.1$ nm for continuous cylindrical defects or $r \geq 1.1$ nm for discontinuous defects. In other metallic materials, radiation-induced defects of minimum radius 2 nm have been directly observed [12], so it is likely that the defects created here by heavy ion irradiation are elongated but noncontinuous. For low fluences ($\phi \leq 5 \times 10^{12}$ ions/cm^2) where ion track overlap is insignificant, the volume of a damaged sample is directly proportional to the fraction ζ, of the track of total length t which is damaged. The volume fraction P' of the damaged sample is

$$P' = \zeta \pi r^2 \phi . \tag{2}$$

From Mössbauer analysis, it is known that $P' = 0.23$ for $\phi = 5 \times 10^{12}$ ions/cm^2; hence

$$r^2 \zeta = 1.5 \times 10^{-18} \text{ m}^{-2}. \tag{3}$$

The influence of irradiation on the 5 K hysteresis loops and virgin magnetization curves is shown in Figs. 2(a) and 2(b). The width of the loop increases greatly with ion fluence. We define the coercive field H_c as the value of external magnetic field at which the irreversible susceptibility is maximum, as this corresponds to the field where the greatest number of magnetic grains reverse their magnetization. Since reversible magnetization processes are expected to be negligible near the coercive field, we make the approximation that $(dM/dH) \approx (dM/dH)^{\text{irr}}$. The coercivity is plotted as a function of the ion fluence in Fig. 2(c). An increase in coercivity of almost 1 order of magnitude is observed for the highest fluence. The initial susceptibility

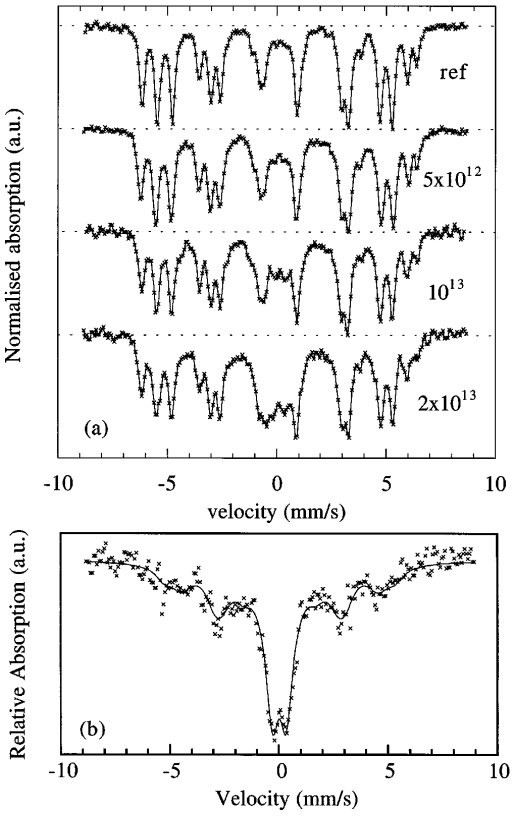

FIG. 1. (a) Room temperature Mössbauer spectra of a reference sample of $Sm_2Fe_{17}N_3$ and samples irradiated with a fluence of 5×10^{12}, 1×10^{13}, and 2×10^{13} Pb ions/cm^2. (b) Room temperature Mössbauer spectrum of the damaged region, for a fluence of 2×10^{13} ions/cm^2, after subtraction of the subspectra for undamaged $Sm_2Fe_{17}N_3$.

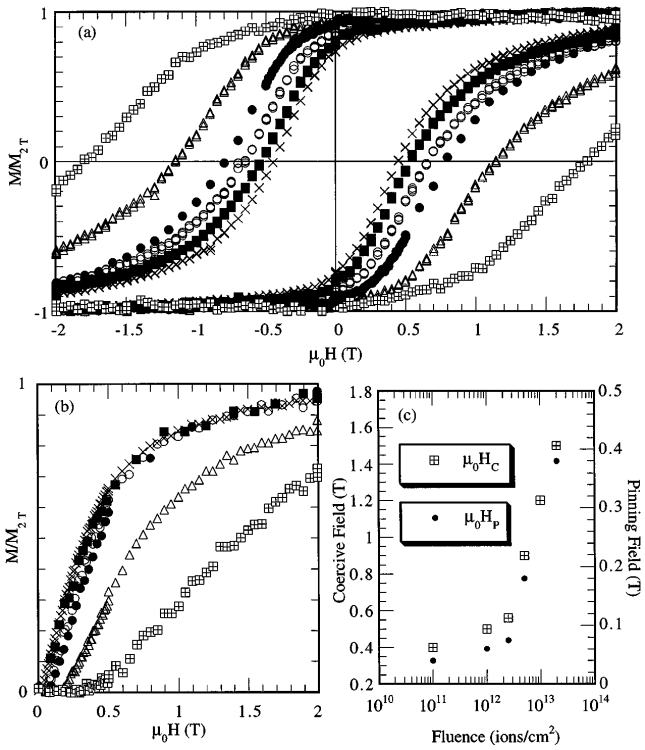

FIG. 2. (a) Hysteresis loops and (b) virgin magnetization curves, measured at 5 K, of a reference sample and irradiated samples of $Sm_2Fe_{17}N_3$; (c) plot of coercive and depinning fields as a function of ion fluence. [(×) nonirradiated; (■) 10^{11}, (○) 10^{12}, (●) 2.5×10^{12}, (△) 5×10^{12}, and (⊞) 2×10^{13} ions/cm^2].

of the reference sample is large in the thermally demagnetized state, as expected for the free motion of domain walls in large multidomain particles. In the irradiated samples however, the initial susceptibility is practically zero until a threshold field is reached. Such behavior in multidomain particles is characteristic of domain wall pinning. The threshold field, H_p, thus corresponds to the minimum field required to depin the domain walls from an irradiation-induced defect. The fluence dependence of Hp is also reported in Fig. 2(c). Both H_c and H_p increase sharply beyond a threshold fluence of 2.5×10^{12} ions/cm^2, which corresponds to an average distance between pinning centers of about 7 nm in the plane perpendicular to the tracks.

The shape of defects introduced by swift heavy ion irradiation depends on the electronic energy loss $(dE/dx)_e$ of the impinging ions. Above the threshold for defect creation, in magnetic insulators [13] and intermetallic targets ($NiZr_2$) [12,14], the defect morphology changes from a string of spherical defects to discontinuous cylindrical defects and finally to continuous defects as $(dE/dx)_e$ increases. In a recent study of the intermetallic YCo_2 system, it was found that high energy (5 GeV) Pb and U ions are just above the threshold value required to create defects [15]; therefore, high thresholds are also expected for other intermetallic systems.

Information on the shape of the defects which have been created in $Sm_2Fe_{17}N_3$ may be obtained from magnetic measurements made parallel and perpendicular to the ion tracks, which are along z. In a sample which is aligned in plane (c axis and domain walls lying perpendicular to the ion tracks) and measured in the easy direction, domain walls traveling in the z direction should only be pinned by spherical or discontinuous defects (Fig. 3). Pinning is not expected for cylindrical defects as the wall will always be at the same energy as it moves up or down the cylindrical tracks. However, in a sample which is aligned out of plane (c axis and domain walls parallel to the ion tracks) and measured in the easy direction, domain walls traveling in the x or y directions will be pinned, whatever the defect shape. Although the above argument is only qualitative, it predicts that for spherical defects the value of coercivity measured is independent of the measuring direction while for elongated defects the coercivity of a sample aligned out of plane should be higher than that of a sample aligned in plane.

The demagnetization curves of anisotropic samples, aligned with the c axes perpendicular or parallel to the ion tracks and measured with the applied field parallel to the c axis, are shown in Fig. 4. The coercivity of the out of plane sample is 50% higher than that measured for the sample aligned in plane, which indicates that the defects pinning the domain walls are highly anisotropic in shape.

In the Kersten model of pinning-type coercivity, a domain wall of area A, interacting with a single pinning site, experiences a restoring force $f(z)$ as the externally applied field drives the wall in the z direction [16]. At some point a critical force f is reached, beyond which the defect can no longer pin the domain wall. The externally applied field at which depinning occurs is H_c and is given by

$$H_c = f/2\mu_0 M_s A\,. \tag{4}$$

To determine H_c it is necessary to know the maximum restoring force of the defect and the area of domain wall which is pinned. Gaunt has considered the problem of domain wall pinning by a random array of point defects [17]. The domain wall is a deformable membrane of surface energy γ, which requires a force to move it over a unit step. In the "strong pinning" regime the domain wall

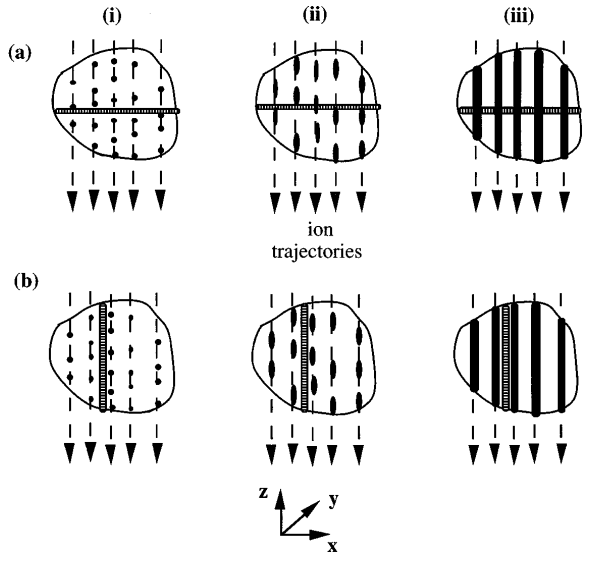

FIG. 3. Hard magnetic grains with (i) spherical, (ii) elongated but discontinuous, and (iii) continuous cylindrical defects aligned (a) in plane and (b) out of plane. The hatched area represents the domain wall which lies parallel to the easy axis of the grain.

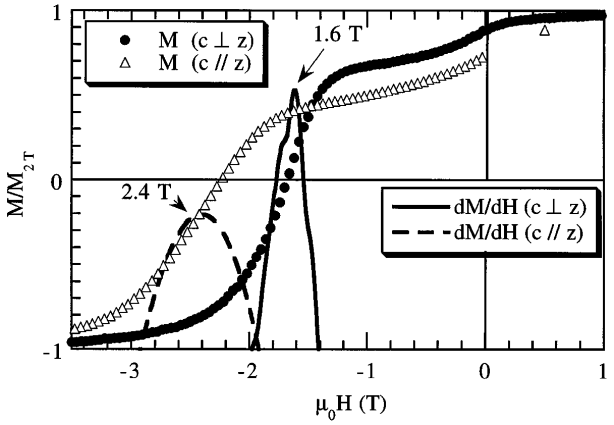

FIG. 4. Low temperature hysteresis loops (10 K) of anisotropic $Sm_2Fe_{17}N_3$ samples aligned in plane or out of plane, irradiated with a fluence of 2×10^{13} Pb ions/cm^2, measured with the applied magnetic field oriented along the easy axis. Also shown are plots of the total susceptibility, dM/dH, from which the coercivity of the hard magnetic phase was determined.

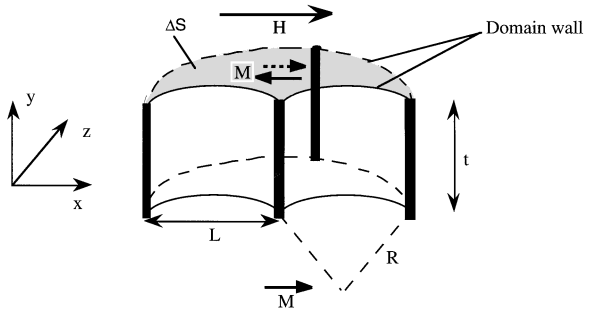

FIG. 5. Breakaway of a domain wall strongly pinned by three coplanar cylindrical defects. The wall bows under the influence of an applied field H, and when H is sufficiently large it breaks away from the central pin. The gray area ΔS is the area swept out, in the plane perpendicular to the defect axes, by the domain wall between breakaway and repinning at another pin. The solid arrow shows the direction of magnetization before breakaway; the dashed arrow shows the direction of magnetization after breakaway.

is depinned from a single defect, and the volume swept out over the unit step contains one replacement pin. Strong pinning arises when $\delta_w \approx 2r$.

We adapt Gaunt's model to the case of strong pinning by cylindrical defects. When elongated discontinuous defects are narrowly separated along the ion track, a domain wall which is parallel to the track will be pinned as for a continuous cylinder of length ζt.

If a domain wall is pinned by three coplanar defects, its depinning from the central defect, under the influence of an external field, and repinning at a new defect constitute a unit step in the magnetization reversal process (Fig. 5). We are concerned with the area, ΔS, swept out by the domain wall in the plane perpendicular to the defects.

$$\Delta S = (1/2)(L^3/R). \tag{5}$$

where L is the distance between the coplanar defects and R is the radius of curvature of the domain wall. Balancing the wall energy and the magnetic energy ($\mu_0 M_S H = \gamma/R$) and using the criterion for strong pinning $\phi \Delta S = 1$ where ϕ is the number of cylindrical defects per unit area, Eq. (5) may be rewritten as

$$L^3 = 2\gamma/\phi\mu_0 M_S H. \tag{6}$$

Substituting the area $A = Lt$ of domain wall per pin into Eq. (4), together with the simplest expression for the restoring force $f \approx \gamma\zeta t$, where ζt is the length of track which is damaged, we find

$$H_c = (1/\mu_0 M_S)(\zeta/2)^{3/2}(\phi/2)^{1/2}\gamma. \tag{7}$$

Taking the slope of the plot of H_c vs $\phi^{1/2}$ for low fluence samples ($\phi < 5 \times 10^{12}$ ions/cm^2), where overlap is insignificant, and substituting it in Eq. (7), we find $\zeta = 0.4$. With this value of ζ, the defect radius deduced from Eq. (3) is 2 nm. While this is only an estimate, it is a very reasonable value in view of the observations of defects created in other intermetallic alloys by heavy ion irradiation. The estimated defect diameter is close to the domain wall width at 4.2 K (2.9 nm), meeting the condition for effective domain wall pinning mentioned earlier.

In conclusion, we have demonstrated that radiation damage induced by swift heavy ions can induce pinning-type coercivity in large particles of a material with strong uniaxial anisotropy. At the highest ion fluence, when the defects occupy half of the particle volume, the coercivity at 5 K is increased fivefold from 0.3 to 1.5 T. Analysis based on magnetic measurements and a model of strong pinning by cylindrical defects indicates that they are elongated and discontinuous disordered regions with a radius of order 2 nm, occupying 40% of the length of the ion track. As the defect geometry is one dimensional, the microstructure can be more effectively controlled by irradiation than by standard metallurgical techniques. This method has considerable potential for further model studies of pinning-type coercivity, but it would only be a practical way for making hard magnets on the micrometer scale.

[1] H. Kronmüller, Phys. Status Solidi B **144**, 385 (1987).
[2] D. Givord and M. F. Rossignol, in *Rare-Earth Iron Permanent Magnets*, edited by J. M. D. Coey (Clarendon Press, Oxford, 1996).
[3] R. K. Mishra, G. Thomas, T. Yoneyama, A. Fukuno, and T. Ojima, J. Appl. Phys. **52**, 2517 (1981).
[4] B. Roas, B. Hensel, S. Henke, S. Klaumunze, B. Kabius, W. Watanabe, G. Saemann-Ischenko, L. Schultz, and K. Urban, Europhys. Lett. **11**, 669 (1990).
[5] J. P. Krumme, I. Bartels, B. Strocka, K. Witter, C. Schmelzer, and R. Spohr, J. Appl. Phys. **48**, 5191 (1977).
[6] D. Givord, J. P. Nozières, M. Ghidini, B. Bervais, and Y. Otani, J. Appl. Phys. **76**, 6661 (1994).
[7] J. M. D. Coey and H. Sun, J. Magn. Magn. Mater. **87**, L251 (1990).
[8] K. Kobayashi, T. Iritama, N. Imaoka, T. Suzuki, H. Kato, and Y. Nakagawa, *Proceedings of the 12th International Workshop on Rare-Earth Magnets and their Applications, Canberra, 1992*, edited by Hi-Perm Lab. (Iowa State University, Ames, Iowa, 1992), p. 32.
[9] J. O'Sullivan, H. Nagel, and J. M. D. Coey, in *Magnetic Hystersis in Novel Magnetic Materials*, edited by G. C. Hadjipanayis (Kluwer, Dordrecht, 1996), p. 669.
[10] J. F. Ziegler and J. P. Bierzack, *The Stopping Range of Ions in Solids* (Pergamon, New York, 1985).
[11] B. P. Hu, H. S. Li, H. Sun, and J. M. D. Coey, J. Phys. Condens. Matter **3**, 3983 (1991).
[12] A. Dunlop and D. Lesueur, Radiat. Eff. Defects Solids **126**, 123 (1993).
[13] F. Studer and M. Toulemonde, Nucl. Instrum. Methods Phys. Res. Sect. B **65**, 560 (1992).
[14] A. Barbu, H. Dammak, A. Dunlop, and D. Lesueur, MRS Bull. **20**, 29 (1995).
[15] J. P. Nozières, M. Ghidini, C. Pinettes, C. Lacroix, B. Gervais, G. Suran, and D. Dufeu, Phys. Rev. B **57**, 57 (1998).
[16] M. Kersten, Phys. Z. **44**, 63 (1943).
[17] P. Gaunt, Philos. Mag. B **48**, 261 (1983).